Atmospheric Environment 263 (2021) 118683

Contents lists available at ScienceDirect

Atmospheric Environment

journal homepage: www.elsevier.com/locate/atmosenv

The nucleation mechanism of succinic acid involved sulfuric acid - Dimethylamine in new particle formation

Zhong-Quan Wang [a,b,c], Yi-Rong Liu [b,**], Chun-Yu Wang [b], Shuai Jiang [b], Ya-Juan Feng [b], Teng Huang [a], Wei Huang [a,b,d,*]

[a] Laboratory of Atmospheric Physico-Chemistry, Anhui Institute of Optics & Fine Mechanics, Hefei Institutes of Physical Science, Chinese Academy of Sciences, Hefei, Anhui, 230031, China
[b] School of Information Science and Technology, University of Science and Technology of China, Hefei, Anhui, 230026, China
[c] Department of Physics, Huainan Normal University, Huainan, Anhui, 232001, China
[d] Center for Excellence in Urban Atmospheric Environment, Institute of Urban Environment, Chinese Academy of Sciences, Xiamen, Fujian, 361021, China

HIGHLIGHTS

- SUA may play an important role in particle formation and growth.
- The SUA molecule is similar to the SA molecule in providing protons to DMA.
- The nucleation mechanism may explain high nucleation rate at low sulfuric acid concentration.

ARTICLE INFO

Keywords:
Nucleation mechanism
Proton transfer
Evaporation rate
Atmospheric relevance

ABSTRACT

Succinic acid (SUA) is a common dicarboxylic acid frequently observed in aerosols. Understanding the role of succinic acid in atmospheric new particle formation is essential to study the complicated nucleation mechanism. In this study, high-precision quantum chemical calculations and atmospheric clusters dynamic code (ACDC) simulations are used to investigate the nucleation mechanism of the $(SA)_x(SUA)_y(DMA)_z$ ($0 = x, y, z \leq 3$) multicomponent system. The most stable molecular structures show that SUA can form relatively stable clusters with the SA-DMA system by hydrogen bond and proton-transfer interactions. Similar to SA molecules, SUA can provide protons to DMA when excess DMA molecules are available. ACDC simulations indicate that SUA can contribute to the cluster formation, especially at low sulfuric acid concentration and high succinic acid concentration. Moreover, the main cluster flux out of the SUA-containing system is along the non-diagonal (the number of acid molecules is greater than that of base molecules), which is different from the pure SA-DMA system. These clusters are stable enough to be present at a fairly high concentration, and could be a platform for growth into the larger sizes. This organic acid involved cluster formation may explain high nucleation rate at low sulfuric acid concentration and high organic acid concentration.

1. Introduction

Atmospheric aerosols have a great influence on health and climate patterns (Kulmala, 2003; Kulmala et al., 2004; Oberdörster and Utell, 2002; Saxon and Diaz-Sanchez, 2005; Zhang et al., 2007). They are usually divided into primary and secondary aerosols according to their formation pathway, i.e., primary aerosols, from natural or anthropogenic, are emitted directly into the atmosphere, while secondary aerosols are produced from gas to particle conversion (Charlson et al., 2001; Claeys et al., 2004, 2007). In the past decades, although many experimental and theoretical works have been performed, the mechanism of secondary aerosols formation has not been well understood (Almeida et al., 2013; Kulmala et al., 2004; Nadykto et al., 2009, 2011; Wang et al., 2010; Wen et al., 2018; Xie et al., 2017; Xu and

* Corresponding author. Laboratory of Atmospheric Physico-Chemistry, Anhui Institute of Optics & Fine Mechanics, Hefei Institutes of Physical Science, Chinese Academy of Sciences, Hefei, Anhui, 230031, China.
** Corresponding author.
E-mail addresses: yrliu@ustc.edu.cn (Y.-R. Liu), huangwei6@ustc.edu.cn (W. Huang).

https://doi.org/10.1016/j.atmosenv.2021.118683
Received 11 June 2021; Received in revised form 12 August 2021; Accepted 13 August 2021
Available online 17 August 2021

Zhang, 2012, 2013; Zhang, 2010; Zhang et al., 2004, 2012, 2013; Zhao et al., 2011). Sulfuric acid (SA) has been identified to be an important precursor (Kulmala et al., 2004; Xie et al., 2017; Zhang et al., 2012; Zhao et al., 2011) of aerosol nucleation through clustering with water (H_2O) (Kulmala et al., 2004), ammonia (NH_3)(Kanakidou et al., 2016; Kirkby et al., 2011), methylamine (MA) (Jen et al., 2014; Lv et al., 2015) and dimethylamine (DMA) (Kürten et al., 2014; Kulmala et al., 2004; Loukonen et al., 2010; Ma et al., 2016). However, the concentration of sulfuric acid in the range of 10^5-10^7 cm^{-3} is not sufficient to explain the actual nucleation rate measured in the atmosphere (Kulmala et al., 2004; Zhang et al., 2012). It is hence suggested that other species are involved in nucleation, such as organic acids (Elm et al., 2017; Hong et al., 2018; Miao et al., 2015; Xu et al., 2010a, 2010b), aldehydes (Kurtén et al., 2015), amino acid (Elm et al., 2013; Wang et al., 2016) and highly oxidized multifunctional organic molecules (HOMs) (Ortega et al., 2015; Zhang et al., 2017). Bianchi et al. (2016) have pointed out that an efficient particle formation and growth requires a high concentration of HOM compounds when the concentration of SA is low. Zhang et al. (2004) have shown that organic acids contribute to aerosol formation by binding to SA.

Recent years have witnessed an increasing number of theoretical studies on the participation of organic acids in the process of atmospheric nucleation (Arquero et al., 2017; Deshmukh et al., 2018; Liu et al., 2017; Wen et al., 2019), with a focus on the thermochemical properties of clusters through the strong hydrogen bond between organic acids and atmospheric nucleation precursors (Han et al., 2018; Miao et al., 2018; Xu and Zhang, 2012). However, the dynamic process and the mechanism of NPF process with the participation of organic acids are still unclear. Dicarboxylic acids, which have a relatively low vapor pressure, are expected to participate in nucleation (Kawamura and Bikkina, 2016; Limbeck et al., 2001; Prenni et al., 2001). Succinic aid (SUA), a common dicarboxylic acid frequently observed in aerosols (Hsieh et al., 2007), is recognized as a precursor species in the NPF. It is mainly produced from volatile organic compounds (VOCs) of anthropogenic and biogenic origin (Kawamura et al., 2013; Kourtchev et al., 2009). Kourtchev et al. (2009) reported the mass concentrations and diel variations for organic tracers in aerosols from K-puszta, Hungay. They found SUA and oxalic acid (OA) participate in SOA formation process, and the concentration of succinic acid was 13.8 ng m^{-3}. Kawamura et al. (2013) measured the high abundances of water-soluble dicarboxylic acids, ketocarboxylic acids and α-dicarbonyls in the mountaintop aerosols over the North China Plain during wheat burning season. This study demonstrates the field burning of agricultural wastes in this region not only controls the high loading of organic aerosols in central East China but also affects the air quality and atmospheric chemistry in the outflow regions of Chinese aerosols in the western North Pacific. They found the concentration of SUA was 7.0–829 ng m^{-3}. Fang et al. (2020) gave the observational evidence for the involvement of dicarboxylic acids (diacids) in particle nucleation. They proposed that diacids could actively participate in particle nucleation and might dominate the initial steps under high [diacids]/[SA] ratios. The signal intensity of the $(SA)_1(SUA)_1(DMA)_1$ cluster was measured by nitrate CI-APi-TOF. On the theoretical side, Xu et al. (Xu and Zhang, 2013) calculated the interaction between succinic acid and dimethylamine. They found strong interactions exist between SUA and DMA by forming of ion pairs, and that the aminium dicarboxylate ion pairs can be formed in the atmosphere by interacting with the dicarboxylic acids combining with amines which contribute to the nucleation of atmospheric nanoparticles. Lin et al. (2019) elucidated the interactions between one SUA molecule and clusters consisting of SA-NH_3/DMA in the presence of hydration of up to six water molecules. Their results indicated that the multicomponent nucleation involved organic acids, sulfuric acid, and base species promotes NPF in the atmosphere, particularly under polluted conditions with a high concentration of diverse organic acids. Previous theoretical research only focused on one SUA molecule involving SA-base clusters. To investigate the dynamic growth of nucleation clusters, it is therefore important to investigate the role of more SUA molecules in the formation of initial clusters and the corresponding participation mechanism to better understand NPF.

In present work, we focus on the mechanism of SUA molecules participated in SA-DMA initial nucleation steps. High-precision quantum chemistry calculations are performed to study the structures and thermodynamics of the $(SA)_x(SUA)_y(DMA)_z$ ($0 = x, y, z \leq 3$) clusters. Geometric and topological analyses are carried out to investigate the binding between SUA and SA-DMA clusters. Atmospheric cluster dynamics code (ACDC) simulations are performed to determine the enhancement effect of SUA on the SA-DMA-based particles formation.

2. Methods

The Basin-Hopping (Huang et al., 2010; Liu et al., 2014; Wales and Doye, 1997; Yoon et al., 2007) algorithm coupled with semiempirical PM7 (Hostaš et al., 2013) implemented in MOPAC 2016 (Wales and Doye, 1997), which has been used to explore atomic and molecular systems in previous studies, is used to search the low-energy structures of $(SA)_x(SUA)_y(DMA)_z$ ($0 = x, y, z \leq 3$). Within this method, new configuration is generated by random displacement of the molecules in the clusters with different Boltzmann temperature (ranging from 3000 to 6000 K) for funnel sampling. For each cluster, four independent BH searches are performed, each for 1000 structures sampling and amounting to 4000 structures. The top 50 isomers, ranking relative to lowest energy structure, are selected to the initial optimized at PW91PW91/6-311 + G (d) level. Then the stable isomers within 10 kcal mol^{-1} relative to lowest energy structures are re-optimized at the PW91PW91/6–311++G (2d, 2p) level, which has been suggested to be more reliable in predicting the SUA and SA-base cluster formation (Lin et al., 2019). In order to make sure the results are consistent, another four methods (B3LYP, M06–2X, ωB97XD and MP2) are performed for the smallest clusters. The results are list in Table S1. It is obviously that the results of PW91PW91 is close to that of MP2. Vibrational frequencies are also calculated to confirm that no imaginary frequencies existed. All the calculations are performed in Gaussian 09 software package (Frisch et al., 2013). Based on the optimized geometries, the single-point energies are calculated at the RI-MP2/cc-pVTZ level of theory using ORCA 4.0 suite of programs (Charlson et al., 2001; Peterson et al., 2008; Yousaf and Peterson, 2008).

The stability of clusters can be significantly affected by the interaction strength. To describe the interaction properties of clusters, a relief map with projection of localized orbital locator (LOL) is generated to describe the occurrence of proton transfer. The LOL value is within the range of 0–1. A large LOL value means that electrons are greatly localized, indicating the existence of a covalent bond. All the parameters were determined in the multifunctional wavefunction analyzer (Multiwfn) 3.3.8 program (Lu and Chen, 2013).

In addition, according to the proton transfer parameter ρ_{PT}(Hunt et al., 2003; Kurnig and Scheiner, 1987), the degree of proton transfer in the hydrogen bond is discussed, and the degree of ionization is evaluated according to the distance between atoms. It includes hydrogen bond shortening and covalent hydrogen bond prolongation of the acid to measure the degree of proton transfer. The formula is as follows:

$$\rho_{PT} = (r_{OH} - r^0_{OH}) - (r_{H\cdots N} - r^0_{H\cdots N}) \quad (1)$$

where, r_{OH} and r^0_{OH} are the O–H distance in SUA or SA and the O–H distance in the free monomer, respectively. $r_{H\cdots N}$ and $r^0_{H\cdots N}$ are the hydrogen bond distances in the SUA-DMA and SA-DMA clusters and the H–N distances in fully protonated DMA, respectively. For a hydrogen bonded cluster, the first term is approximately zero and ρ_{PT} is negative. The second term is zero, and ρ_{PT} is positive for the cluster with protons completely transferred to dimethylamine. The value of ρ_{PT} is close to zero, which means that the proton sharing between acid and base is equal.

Collision and evaporation between clusters were studied by the Atmospheric Cluster Dynamics Code (ACDC) simulation (McGrath et al., 2012). The birth-death equations are as follows:

$$\frac{dc_i}{dt} = \frac{1}{2}\sum_{j<i}\beta_{j,(i-j)}c_j c_{(i-j)} + \sum_j \gamma_{(i+j)\to i}c_{i+j} - \sum_j \beta_{i,j}c_i c_j - \frac{1}{2}\sum_{j<i}\gamma_{i\to j}c_i + Q_i - S_i \quad (2)$$

where c_i is the concentration of cluster i, β_{ij} is the collision coefficient of clusters i with j, and $\gamma_{(i+j)\to j}$ is the evaporation coefficient of cluster $i+j$ evaporating into clusters i and j. Q_i is the possible additional source of cluster i and S_i is the sink term of cluster i.

The collision coefficients are taken from the kinetic gas theory, and the evaporation coefficient is calculated from Gibbs free energies of formation of mother and daughter cluster.

$$\gamma_{(i+j)\to i} = \beta_{ij}\frac{c_i^e c_j^e}{c^e{}_{i+j}} = \beta_{ij}c_{\mathrm{ref}}\exp\left(\frac{\Delta G_{i+j} - \Delta G_i - \Delta G_j}{k_b T}\right) \quad (3)$$

where β_{ij} is the collision coefficient between clusters i and j, c_i^e is the equilibrium concentration of cluster i, ΔG is the Gibbs free energy of the formation of cluster i, and c_{ref} is the monomer concentration of the reference vapor corresponding to the pressure of 1 atm at which the Gibbs free energies were determined.

3. Results and discussion

3.1. Structures and topology

In this calculation, there are 58 low energy structures of the $(SA)_x(SUA)_y(DMA)_z$ ($0 = x, y, z \le 3$) systems. The xyz coordinates of all the studied clusters are listed in the supplementary data.

Fig. 1 shows the global minimum energy structures of the $(SA)_x(SUA)_y(DMA)_z$ ($1 \le z \le x + y \le 3$) clusters. With the increase of molecular number, the structures of all the clusters gradually change from ring structure to cage structure. SUA molecules can form relatively stable clusters with the SA-DMA system by hydrogen bonding and proton-transfer interactions. SA and SUA molecules can transfer a proton to the nitrogen of DMA, forming $[HSO4]^-[HCH_3NCH_3]^+$ and $[H_5C_4O_4]^-[HCH_3NCH_3]^+$ ion pairs. Thus, the SUA molecule can be similar to the SA molecule in providing protons to DMA.

We compare the structures of SA-SUA-DMA-base clusters to the corresponding binary SA-DMA-based clusters. LBO of the newly formed covalent bond via proton transfer are calculated. The optimized structures and the corresponding LOL distribution maps of the most stable $(SA)_2(DMA)_1$ and $(SA)_1(SUA)_1(DMA)_1$ clusters are shown in Fig. 2. It can be observed that SA, DMA and SUA molecules interact with each other through hydrogen bonds. In these two clusters, the red area between H1–N1 and green area between H1–O1 indicate that a proton transfers from SA to DMA. Proton transfer converts the N1–H1 hydrogen bonding to a covalent bond, leading to the formation of the dimethylamine bisulfate ion pair, with LBO value of 0.593 for $(SA)_2(DMA)_1$ cluster and 0.548 for $(SA)_1(SUA)_1(DMA)_1$ cluster. As shown in Table 1, the electron density ρ at BCPs of bond H1–N1 in $(SA)_2(DMA)_1$ and $(SA)_1(SUA)_1(DMA)_1$ clusters are 0.309 a.u. and 0.298 a.u. respectively. Other SUA-contained clusters as shown in Fig. S1 and Fig. S2.

In conclusion, SUA plays a significant role in forming relatively stable clusters with SA-DMA system through interactions by hydrogen bond and proton-transfer. SUA molecule is similar to SA molecule in providing protons to DMA when excess DMA molecules are available. The result indicates that SUA may play an important role in particle formation and growth when the concentration of SA is low.

3.2. Thermochemical analysis

The nucleation mechanism is very important in the study of atmospheric aerosols, and the nucleation rate is closely related to the free energy. The Gibbs free energies of formation ΔG of all the most stable clusters at temperatures of 278 K are listed in Table S2. Fig. 3 shows the cluster formation Gibbs free energies (ΔG) of $(SA)_x(SUA)_y(DMA)_z$ ($x + y \le 3$, $1 = z \le 3$) at 278 K. The different colors represent the different number of SUA molecules, that is, zero (black circle), one (red circle), two (green circle), three (blue circle). The clusters show that with the same number of DMA molecules and acid (SA or SUA) molecules, the ΔG of the SA-DMA system is lowest, and the ΔG of the SUA-DMA system is highest. For ternary SA-SUA-DMA clusters with the same number of base molecules, the ΔG of clusters with more acidic molecules are lower than

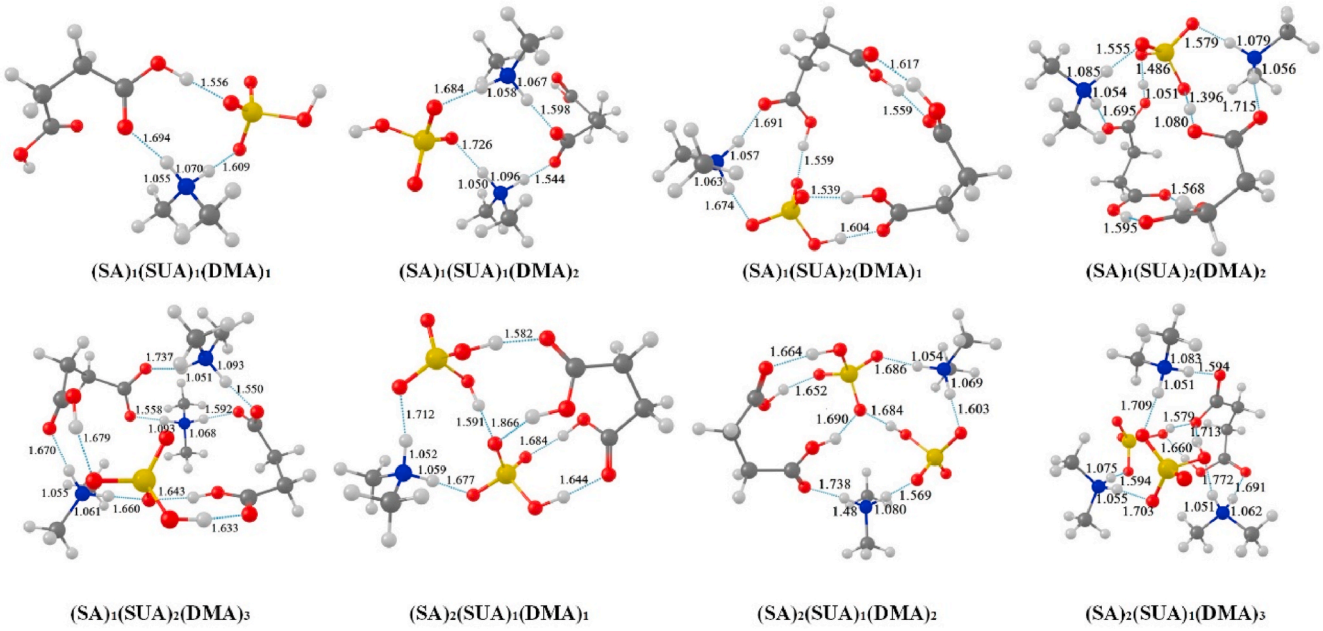

Fig. 1. The most stable structures of $(SA)_x(SUA)_y(DMA)_z$ ($1 \le z \le x + y \le 3$) clusters calculated at the PW91PW91/6–311++G (2d, 2p) level. The red, yellow, blue, white and black balls represent O, S, N, H and C atoms, respectively. The lengths of the hydrogen bonds shown in dashed lines are given in Å. (For interpretation of the references to color in this figure legend, the reader is referred to the Web version of this article.)

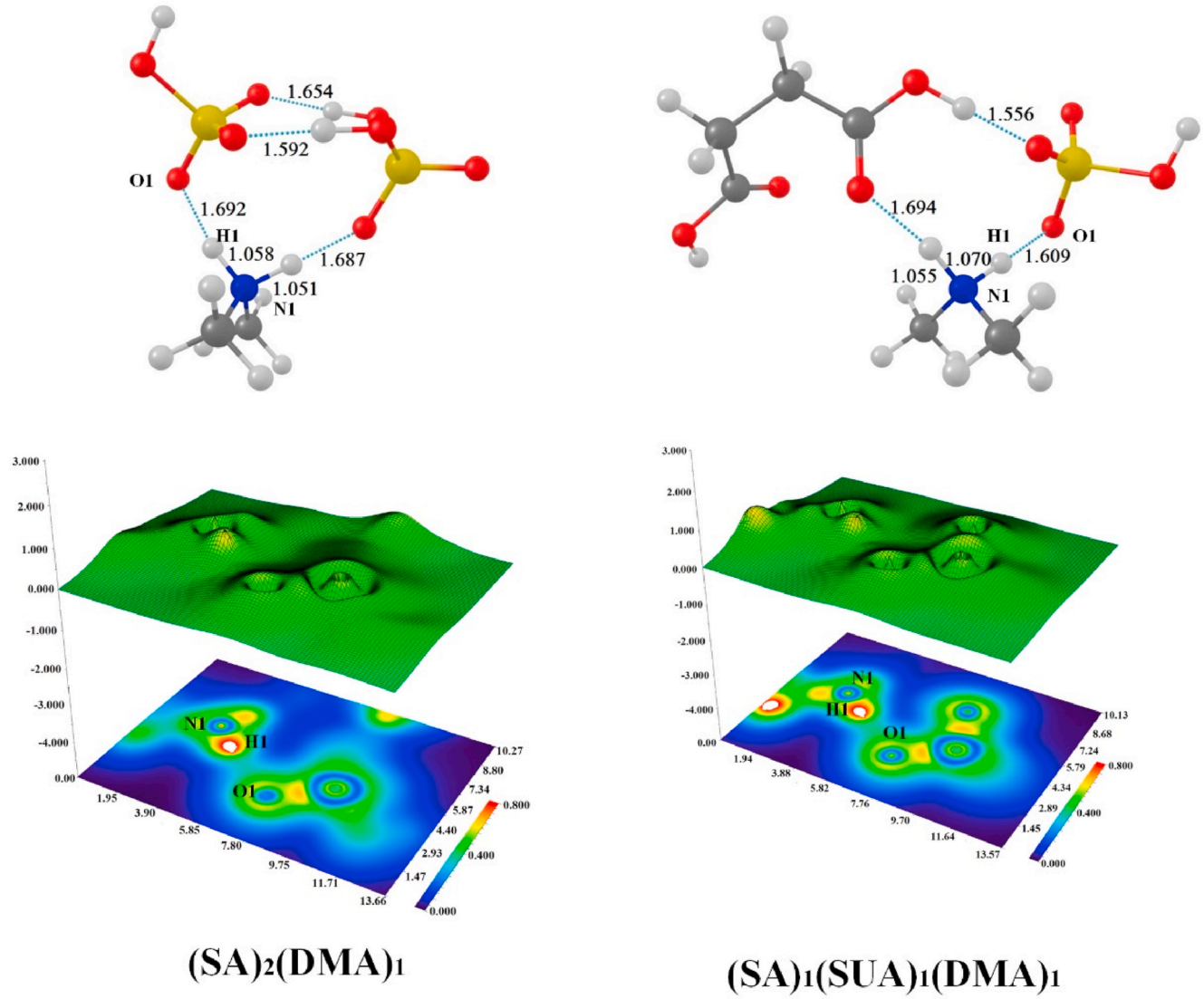

Fig. 2. Most stable structures and corresponding LOL distribution maps of $(SA)_2(DMA)_1$ and $(SA)_1(SUA)_1(DMA)_1$ clusters. The hydrogen bonds are shown as dashed lines and given in Å.

Table 1
Proton-transfer parameter (ρ_{PT}/Å) and the Laplacian bond order (LBO) (a.u.) of the nitrogen-hydrogen bond in the clusters. The total number of proton transfers (n) and the proton donor and acceptor are also listed.

Cluster	r_{OH}	r_{N-H}	ρ_{PT}	LBO	Proton donor	Proton acceptor	n
$(SA)_2(DMA)_1$	1.692	1.058	0.695	0.593	SA	DMA	1
$(SA)_1(SUA)_1(DMA)_1$	1.609	1.609	0.600	0.548	SA	DMA	1
$(SA)_2(DMA)_2$	1.727	1.051	0.737	0.614	SA	DMA	2
	1.612	1.072	0.593	0.549	SUA	DMA	
$(SA)_1(SUA)_1(DMA)_2$	1.684	1.058	0.687	0.593	SA	DMA	2
	1.544	1.096	0.501	0.478	SUA	DMA	
$(SA)_3(DMA)_3$	1.752	1.055	0.758	0.608	SA	DMA	3
	1.660	1.060	0.661	0.589	SA	DMA	
	1.680	1.063	0.678	0.582	SA	DMA	
$(SA)_2(SUA)_1(DMA)_3$	1.691	1.062	0.690	0.589	SA	DMA	3
	1.594	1.075	0.580	0.537	SA	DMA	
	1.594	1.083	0.564	0.489	SUA	DMA	
$(SA)_1(SUA)_2(DMA)_3$	1.660	1.061	0.660	0.580	SA	DMA	3
	1.558	1.093	0.518	0.483	SUA	DMA	
	1.550	1.093	0.510	0.486	SUA	DMA	

that of clusters with fewer acidic molecules, for instance, the ΔG of the $(SA)_2(SUA)_1(DMA)_2$ cluster is lower than that of the $(SA)_1(SUA)_1(DMA)_2$ cluster. In addition, for clusters with the same number of acidic and basic molecules, the more SA molecules in the cluster, the lower the free energy is. For example, the ΔG of the $(SA)_2(SUA)_1(DMA)_3$ cluster is lower than that of $(SA)_1(SUA)_2(DMA)_3$

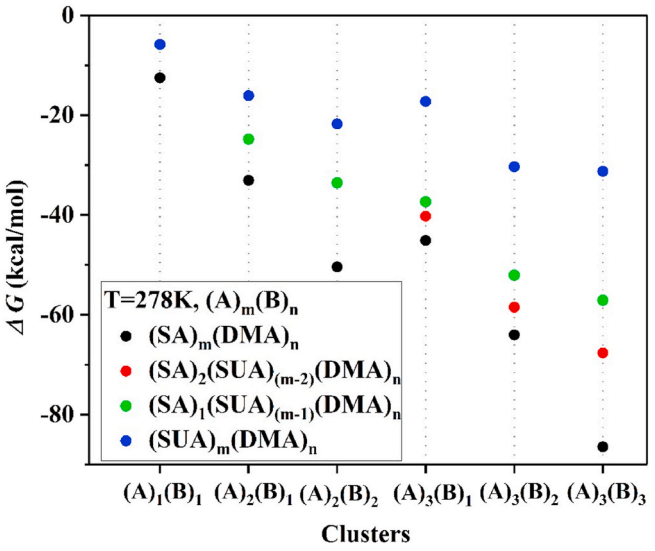

Fig. 3. Formation free energies (ΔG, kcal mol^{-1}) of mA.nB clusters (A=$(SA)_x(SUA)_y$, B = $(DMA)_z$, x + y ≤ 3, 1 = z ≤ 3 and x + y = m, z = n) at 278 K.

cluster. The result indicates that the nucleation in the initial stage may be dominated by SA and DMA acid-base nucleation mechanisms. Thus, SUA may contribute to the cluster growth, especially at low sulfuric acid concentration and high dimethylamine concentration.

3.3. Atmospheric cluster dynamics simulation

3.3.1. Mechanism of new particle formation

The clustering pathway is an important way to understand the mechanism of cluster formation. The flux is the formation rate of the cluster ($i + j$) that equals the collision rate between molecules/clusters i and j minus the evaporation rate of the cluster ($i + j$). Fig. 4 shows the main growth pathways of the clusters involving SUA growing out of the simulation system have been studied at 278 K. The condition is consistent with the simulation where [SA] = 1×10^6 cm^{-3}, [SUA] = 5×10^8 cm^{-3} and [DMA] = 50 ppt, which are the median values of the concentration observed in the field outside by Fang et al., (2020), respectively.

As shown in Fig. 4, the growth path of pure SA-DMA system is the same tendency as that of previous studies. The cluster $(SA)_1(DMA)_1$ is the first step, then SA-DMA grows along diagonal to form $(SA)_2(DMA)_2$ or collides with SA monomer to form $(SA)_2(DMA)_1$ and then collides with DMA to form $(SA)_2(DMA)_2$ at last. For $(SA)_3(DMA)_3$ cluster, the pathway is the same with that of $(SA)_2(DMA)_2$ cluster.

The cluster growth in the SUA-containing system is different from the pure SA-DMA system. The first step is $(SA)_1(DMA)_1$+SUA→ $(SA)_1(SUA)_1(DMA)_1$. Then, one SUA molecule added to $(SA)_1(SUA)_1(DMA)_1$ cluster to form the $(SA)_1(SUA)_2(DMA)_1$ cluster. This path is different from that of pure SA system with acid-base ratio of 2:2. After that a DMA molecule add to $(SA)_1(SUA)_2(DMA)_1$ cluster. For the $(SA)_2(SUA)_2(DMA)_3$ cluster, 94.28% contribution through the path of add a $(SA)_1(DMA)_1$ cluster to $(SA)_1(SUA)_2(DMA)_2$. It shows that the collision between cluster and cluster to form bigger cluster is the main pathway. The other pathway in the SUA-containing system is added a

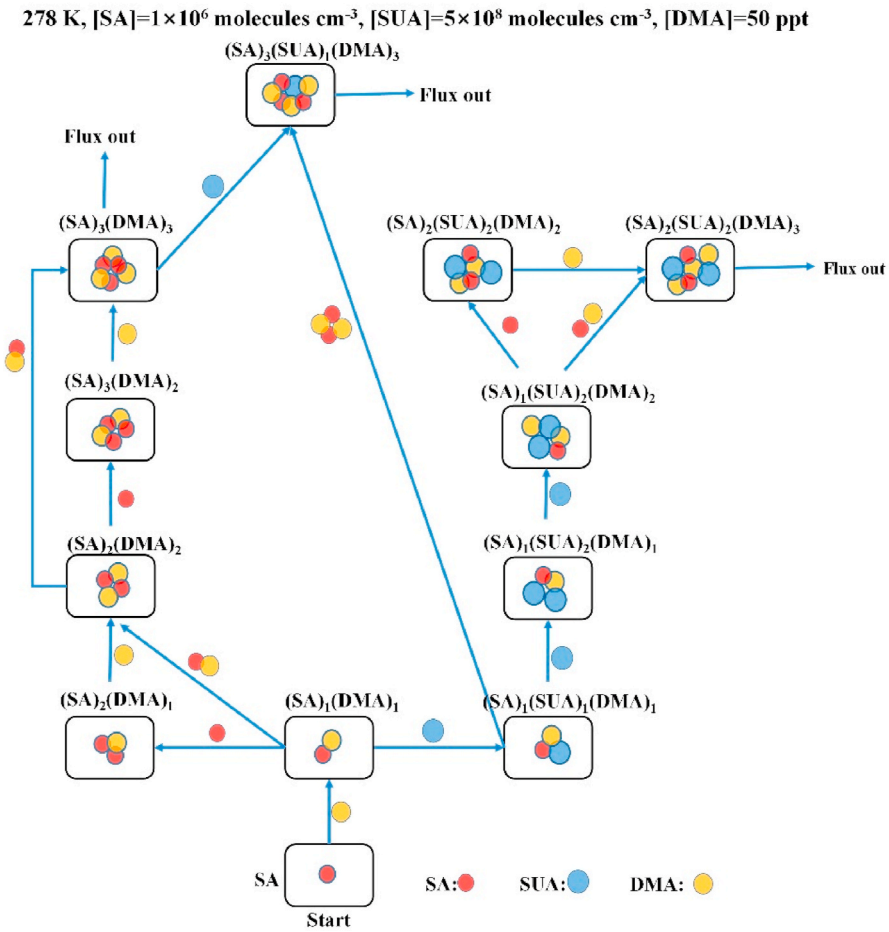

Flux to $(SA)_1(DMA)_1$:	
SA + DMA	100%
Flux to $(SA)_2(DMA)_1$:	
$(SA)_1(DMA)_1$ + SA	100%
Fluxes to $(SA)_2(DMA)_2$:	
$(SA)_2(DMA)_1$ + DMA	61.14%
$(SA)_1(DMA)_1$ + $(SA)_1(DMA)_1$	38.85%
Others	0.01%
Fluxes to $(SA)_3(DMA)_2$:	
$(SA)_2(DMA)_2$ + SA	98.74%
Others	1.26%
Fluxes to $(SA)_3(DMA)_3$:	
$(SA)_3(DMA)_2$ + DMA	55.43%
$(SA)_2(DMA)_2$ + $(SA)_1(DMA)_1$	44.55%
Others	0.02%
Fluxes to $(SA)_3(SUA)_1(DMA)_3$:	
$(SA)_3(DMA)_3$ + SUA	91.76%
$(SA)_2(DMA)_2$ + $(SA)_1(SUA)_1(DMA)_1$	8.22%
Others	0.02%
Fluxes to $(SA)_1(SUA)_1(DMA)_1$:	
$(SA)_1(DMA)_1$ + SUA	99.93%
Others	0.07%
Fluxes to $(SA)_1(SUA)_2(DMA)_1$:	
$(SA)_1(SUA)_1(DMA)_1$ + SUA	99.87%
Others	0.13%
Fluxes to $(SA)_1(SUA)_2(DMA)_2$:	
$(SA)_1(SUA)_2(DMA)_1$ + DMA	99.92%
Others	0.08%
Fluxes to $(SA)_2(SUA)_2(DMA)_2$:	
$(SA)_1(SUA)_2(DMA)_2$ + SA	92.92%
$(SA)_1(SUA)_2(DMA)_1$ + $(SA)_1(DMA)_1$	3.75%
Others	3.33%
Fluxes to $(SA)_2(SUA)_2(DMA)_3$:	
$(SA)_1(SUA)_2(DMA)_2$ + $(SA)_1(DMA)_1$	94.28%
$(SA)_2(SUA)_2(DMA)_2$ + DMA	5.71%
Others	0.01%
Fluxes out:	
$(SA)_3(SUA)_1(DMA)_3$	56.43%
$(SA)_2(SUA)_2(DMA)_3$	43.57%

Fig. 4. Main cluster formation pathways at T = 278 K with the concentration of [SA] = 1×10^6 cm^{-3}, [SUA] = 5×10^8 cm^{-3} and [DMA] = 50 ppt.

SUA molecule to the $(SA)_3(DMA)_3$ cluster form the $(SA)_3(SUA)_1(DMA)_3$ cluster. For the $(SA)_3(SUA)_1(DMA)_3$ cluster, 91.76% contribution through the path of add a SUA molecule to $(SA)_3(DMA)_3$.

The main path of the SUA-containing system is along the non-diagonal (the number of acid molecules is greater than that of base molecules), which is different from the pure SA-DMA system. Clusters' total evaporation rates shown in Fig. 5 might be responsible for it. The evaporation rates on different evaporation paths are list in Table S3. As show in Fig. 5, the smaller evaporation rate occurs in the cluster with acid-base ratio of 1:1, followed by the system with acid larger than base in the pure SA-DMA system. Thus, the main path in the pure SA-DMA system is added a SA molecule first and then added a DMA molecule, or added a $(SA)_1(DMA)_1$ cluster to form the larger cluster. For the SUA-containing system, the smaller evaporation rate occurs in the cluster with number of acid molecule lager than number of DMA molecule. When the number of base molecules in the cluster is larger than that of acid molecules, the cluster has a large evaporation rate, which is the same as the SA-DMA system. Different from SA-DMA system, when the clusters have the same number of acid and base molecules, the evaporation rate is also large. The main evaporation path is DMA monomer evaporate from the cluster.

3.3.2. Formation rate of the SA-SUA-DMA system

The formation rate of clusters is an important parameter of NPF. The ACDC simulation is performed in the range of atmospheric precursor concentrations to calculate the formation rate (J) in the SA-SUA-DMA system. In ACDC simulation, the unstable clusters will evaporate back to smaller clusters. While others will continue to grow and grow out of the studied system. From the growth in the SUA-containing system, it can be seen that clusters with 4 acids and 3 base are stable enough and hence allowed to grow out of the simulated system. The way to check if the "box size" is sufficiently large is to compare the ratio of the collision and evaporation rates of the clusters at the boundary of the "box" included in the simulation (Besel et al., 2020). If this ratio is » 1 for at least some of the clusters, then the box size is sufficiently large. Table S4 list the ratio of the collision and evaporation rates of the clusters at the boundary of the "box". Thus, the boundary of the "box" is set at "4 × 3 ″, where 4 is the total number of acid molecules and 3 is the number of amine molecules in the cluster. The condensation sink coefficient is set to 1.5×10^{-3} s^{-1}, which is an average value from observations (Fang et al., 2020). The maximum cluster size is approximately 1.2 nm.

Fig. 6 shows the theoretical nucleation expectations of SA-DMA and SA-SUA-DMA system. The SA concentration is range from 3×10^5 to 10^8 molecules cm^{-3}. The measured formation rates of SA-DMA (black squares) in the CERN-CLOUD experiments (Almeida et al., 2013) are

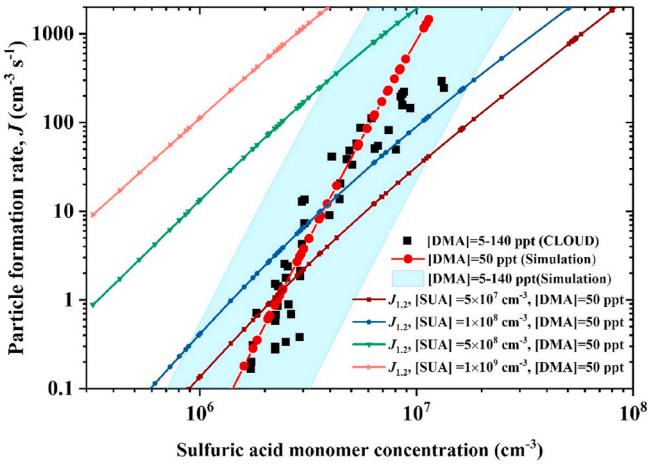

Fig. 6. Formation rates of the SA-SUA-DMA system vs the concentration of SA and comparison with SA-DMA in the CERN-CLOUD experiments at 278 K. The CLOUD data is measured with [DMA] = 5–140 ppt. The red line is the theoretical expectation of SA-DMA system with [DMA] = 50 ppt. The blue bands corresponds to the formation rates of SA-DMA with the concentration of DMA range from 5 to 140 ppt. The other colored lines are the formation rates of SA-SUA-DMA with different concentration of SUA and [DMA] = 50 ppt. (For interpretation of the references to color in this figure legend, the reader is referred to the Web version of this article.)

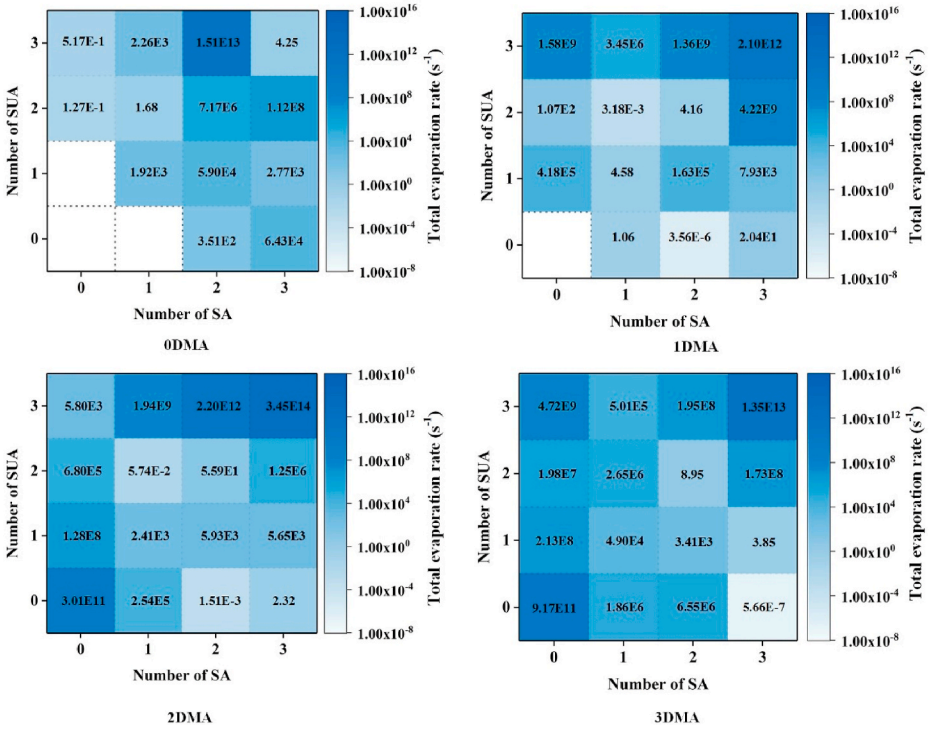

Fig. 5. The total evaporation rates for the $(SA)_x(SUA)_y(DMA)_z$ ($0 \leq x, y, z \leq 3$) clusters with different DMA numbers on the SA-SUA grid at 278 K.

also show in Fig. 6. The concentrations of DMA is range from 5 to 140 ppt. For the SA-DMA system, the simulation system is a "5 × 5 box", where 5 is the maximum number of acid or amine molecules in the cluster. The xyz coordinates of all the clusters are listed in the supplementary data, and the Gibbs free energies of formation ΔG are list in Table S2. In Fig. 6, the blue bands corresponds to the formation rates of SA-DMA system with the concentration of DMA range from 5 to 140 ppt. The red line is the theoretical expectation of SA-DMA system with [DMA] = 50 ppt. The results of theoretical simulation are in agreement with the experimental results.

For the SA-SUA-DMA system, the formation rates are calculated at different concentration of SUA and DMA. The concentration is range from 5×10^7 to 10^9 molecules cm^{-3} to SUA and set 50 ppt to DMA, which are in the range of the concentration observed in the field outside (Fang et al., 2020; Zhang et al., 2012). As show in Fig. 6, the linear slope of formation rate of the SA-SUA-DMA system is lower than that of the SA-DMA system. At low concentration of SUA (5×10^7 and 1×10^8 molecules cm^{-3}), the nucleation rate of SA-SUA-DMA system is higher than that of SA-DMA system at low concentration of sulfuric acid, and lower than that of SA-DMA system at high concentration of sulfuric acid. When increases the concentration of SUA, the formation rate increases rapidly. It is worth noting that the formation rates of the SA-SUA-DMA system corresponds to the cluster size of 1.2 nm. The formation rate for the smaller size may be overestimated. Thus, if the cluster size is extended to 1.7 nm, the corresponding nucleation rate will be smaller. However, it does not affect the conclusion that SUA can participate in the nucleation and promote the growth of SA-DMA system.

In summary, the SA-SUA-DMA system plays a substantial role in the new particle formation. The cluster growth path in the SUA-containing system is different from the pure SA-DMA system. The main path of the SUA-containing system is along the non-diagonal (the number of acid molecules is greater than that of base molecules). At low concentration of SUA (5×10^7 and 1×10^8 molecules cm^{-3}), the nucleation rate of SA-SUA-DMA system is higher than that of SA-DMA system at low concentration of sulfuric acid, and lower than that of SA-DMA system at high concentration of sulfuric acid. When increases the concentration of SUA, the formation rate increases rapidly. This organic acid involved cluster formation may explain high nucleation rate at low sulfuric acid concentration and high organic acid concentration.

4. Conclusions

In this paper, the mechanism of SUA in the atmospheric particle formation of $(SA)_x(SUA)_y(DMA)_z$ ($0 = x, y, z \leq 3$) systems was investigated. For the stable conformation of all the ternary SA-SUA-DMA clusters, SA, DMA and SUA molecules form cyclic ring structures through hydrogen bonds. Proton transfer occurs in all ternary SA-SUA-DMA clusters. When the SA molecule is more abundant than the DMA molecule, the SA molecule is the proton donor. Once there is an additional DMA molecule in the clusters, the SUA molecule can provide protons to the remaining DMA molecules. Therefore, the SUA molecule is similar to the SA molecule in providing protons to DMA when excess DMA molecules are available.

An ACDC simulation was performed to study the clustering pathway and formation rate of the SA-SUA-DMA system. The main path of the SUA-containing system is along the non-diagonal (the number of acid molecules is greater than that of base molecules), which is different from the pure SA-DMA system. At low concentration of SUA (5×10^7 and 1×10^8 molecules cm^{-3}), the nucleation rate of SA-SUA-DMA system is higher than that of SA-DMA system at low concentration of sulfuric acid, and lower than that of SA-DMA system at high concentration of sulfuric acid. When increases the concentration of SUA, the formation rate increases rapidly. This organic acid involved cluster formation may explain high nucleation rate at low sulfuric acid concentration and high organic acid concentration.

This work provides a readily available instrument for understanding the participant mechanism of SUA in the atmospheric particle formation of SA-DMA systems. SUA molecules could actively participate in nucleation and act as proton donors to form stable clusters with SA-base, thus promoting the formation of NPF. Further studies will be conducted to evaluate the role of different organic acids with distinct functionalities in NPF.

CRediT authorship contribution statement

Zhong-Quan Wang: Conceptualization, Methodology, Data curation, Writing – original draft, Writing – review & editing. **Yi-Rong Liu:** Methodology, Validation, Formal analysis, Writing – review & editing. **Chun-Yu Wang:** Formal analysis, Data curation. **Shuai Jiang:** Software, Investigation, Visualization. **Ya-Juan Feng:** Visualization. **Teng Huang:** Resources. **Wei Huang:** Methodology, Software, Supervision, Project administration, Funding acquisition.

Declaration of competing interest

There are no conflicts of interest to declare.

Acknowledgments

This work was supported by the National Science Fund for Distinguished Young Scholars (Grant No. 41725019), the National Key Research and Development Program (Grant No. 2016YFC0202203), the National Natural Science Foundation of China (Grant Nos. 41775122, 41605099, 41705097, 41705111, 41877305 and 41527808), the Key Research Program of Frontier Science, CAS (Grant No. QYZDB-SSW-DQC031), the National Research Program for Key Issues in Air Pollution Control (DQGG0103) and the Fundamental Research Funds for the Central Universities (Grant No. WK2100000008).

Appendix A. Supplementary data

Supplementary data to this article can be found online at https://doi.org/10.1016/j.atmosenv.2021.118683.

References

Almeida, J., Schobesberger, S., Kuerten, A., Ortega, I.K., et al., 2013. Molecular understanding of sulphuric acid-amine particle nucleation in the atmosphere. Nature 502, 359–363.
Arquero, K.D., Gerber, R.B., Finlayson-Pitts, B.J., 2017. The role of oxalic acid in new particle formation from methanesulfonic acid, methylamine, and water. Environ. Sci. Technol. 51, 2124–2130.
Besel, V., Kubečka, J., Kurtén, T., Vehkamäki, H., 2020. Impact of quantum chemistry parameter choices and cluster distribution model settings on modeled atmospheric particle formation rates. J. Phys. Chem. A 124, 5931–5943.
Bianchi, F., Tröstl, J., Junninen, H., Frege, C., et al., 2016. New particle formation in the free troposphere: a question of chemistry and timing. Science 352, 1109.
Charlson, R.J., Seinfeld, J.H., Nenes, A., Kulmala, M., Laaksonen, A., Facchini, M.C., 2001. Reshaping the theory of cloud formation. Science 292, 2025.
Claeys, M., Graham, B., Vas, G., Wang, W., et al., 2004. formation of secondary organic aerosols through photooxidation of isoprene. Science 303, 1173.
Claeys, M., Szmigielski, R., Kourtchev, I., Van der Veken, P., Vermeylen, R., Maenhaut, W., Jaoui, M., Kleindienst, T.E., Lewandowski, M., Offenberg, J.H., Edney, E.O., 2007. Hydroxydicarboxylic Acids: markers for secondary organic aerosol from the photooxidation of α-pinene. Environ. Sci. Technol. 41, 1628–1634.
Deshmukh, D.K., Mozammel Haque, M., Kawamura, K., Kim, Y., 2018. Dicarboxylic acids, oxocarboxylic acids and α-dicarbonyls in fine aerosols over central Alaska: implications for sources and atmospheric processes. Atmos. Res. 202, 128–139.
Elm, J., Fard, M., Bilde, M., Mikkelsen, K.V., 2013. Interaction of Glycine with common atmospheric nucleation precursors. J. Phys. Chem. A 117, 12990–12997.
Elm, J., Myllys, N., Olenius, T., Halonen, R., Kurtén, T., Vehkamäki, H., 2017. Formation of atmospheric molecular clusters consisting of sulfuric acid and C8H12O6 tricarboxylic acid. Phys. Chem. Chem. Phys. 19, 4877–4886.
Fang, X., Hu, M., Shang, D., Tang, R., Shi, L., et al., 2020. Observational evidence for the involvement of dicarboxylic acids in particle nucleation. Environ. Sci. Technol. Lett. 7, 388–394.
Frisch, M.J., Trucks, G.W., Schlegel, H.B., Scuseria, G.E., Robb, M.A., Cheeseman, J.R., Scalmani, G., Barone, et al., 2013. Gaussian 09 Rev. D.01. Gaussian. *Inc.*, Wallingford, CT.

Han, Y.-J., Feng, Y.-J., Miao, S.-K., Jiang, S., Liu, Y.-R., Wang, C.-Y., Chen, J., Wang, Z.-Q., Huang, T., Li, J., Huang, W., 2018. Hydration of 3-hydroxy-4,4-dimethylglutaric acid with dimethylamine complex and its atmospheric implications. Phys. Chem. Chem. Phys. 20, 25780–25791.
Hong, Y., Liu, Y.-R., Wen, H., Miao, S.-K., Huang, T., Peng, X.-Q., Jiang, S., Feng, Y.-J., Huang, W., 2018. Interaction of oxalic acid with methylamine and its atmospheric implications. RSC Adv. 8, 7225–7234.
Hostaš, J., Řezáč, J., Hobza, P., 2013. On the performance of the semiempirical quantum mechanical PM6 and PM7 methods for noncovalent interactions. Chem. Phys. Lett. 568–569, 161–166.
Hsieh, L.-Y., Kuo, S.-C., Chen, C.-L., Tsai, Y.I., 2007. Origin of low-molecular-weight dicarboxylic acids and their concentration and size distribution variation in suburban aerosol. Atmos. Environ. 41, 6648–6661.
Huang, W., Pal, R., Wang, L.-M., Zeng, X.C., Wang, L.-S., 2010. Isomer identification and resolution in small gold clusters. J. Chem. Phys. 132.
Hunt, S.W., Higgins, K.J., Craddock, M.B., Brauer, C.S., Leopold, K.R., 2003. Influence of a polar near-neighbor on incipient proton transfer in a strongly hydrogen bonded complex. J. Am. Chem. Soc. 125, 13850–13860.
Jen, C.N., McMurry, P.H., Hanson, D.R., 2014. Stabilization of sulfuric acid dimers by ammonia, methylamine, dimethylamine, and trimethylamine. J. Geophys. Res. Atmos. 119, 7502–7514.
Kanakidou, M., Myriokefalitakis, S., Daskalakis, N., Fanourgakis, G., Nenes, A., Baker, A. R., Tsigaridis, K., Mihalopoulos, N., 2016. Past, present, and future atmospheric nitrogen deposition. J. Aerosol Sci. 73, 2039–2047.
Kawamura, K., Bikkina, S., 2016. A review of dicarboxylic acids and related compounds in atmospheric aerosols: molecular distributions, sources and transformation. Atmos. Res. 170, 140–160.
Kawamura, K., Tachibana, E., Okuzawa, K., Aggarwal, S.G., Kanaya, Y., Wang, Z.F., 2013. High abundances of water-soluble dicarboxylic acids, ketocarboxylic acids and α-dicarbonyls in the mountaintop aerosols over the North China Plain during wheat burning season. Atmos. Chem. Phys. 13, 8285–8302.
Kirkby, J., Curtius, J., Almeida, J., Dunne, E., er, al, 2011. Role of sulphuric acid, ammonia and galactic cosmic rays in atmospheric aerosol nucleation. Nature 476, 429–433.
Kourtchev, I., Copolovici, L., Claeys, M., Maenhaut, W., 2009. Characterization of atmospheric aerosols at a forested site in central europe. Environ. Sci. Technol. 43, 4665–4671.
Kürten, A., Jokinen, T., Simon, M., Sipilä, M., et al., 2014. Neutral molecular cluster formation of sulfuric acid–dimethylamine observed in real time under atmospheric conditions. Proc. Natl. Acad. Sci. U.S.A. 111, 15019–15024.
Kulmala, M., 2003. How particles nucleate and grow. Science 302, 1000–1001.
Kulmala, M., Vehkamaki, H., Petaja, T., Dal Maso, M., Lauri, A., Kerminen, V.M., Birmili, W., McMurry, P.H., 2004. Formation and growth rates of ultrafine atmospheric particles: a review of observations. J. Aerosol Sci. 35, 143–176.
Kurnig, I.J., Scheiner, S., 1987. Ab Initio investigation of the structure of hydrogen halide-amine complexes in the gas phase and in a polarizable medium. Int. J. Quant. Chem. 32, 47–56.
Kurtén, T., Elm, J., Prisle, N.L., Mikkelsen, K.V., Kampf, C.J., Waxman, E.M., Volkamer, R., 2015. Computational study of the effect of glyoxal–sulfate clustering on the henry's law coefficient of glyoxal. J. Phys. Chem. A 119, 4509–4514.
Limbeck, A., Puxbaum, H., Otter, L., Scholes, M.C., 2001. Semivolatile behavior of dicarboxylic acids and other polar organic species at a rural background site (Nylsvley, RSA). Atmos. Environ. 35, 1853–1862.
Lin, Y., Ji, Y., Li, Y., Secrest, J., Xu, W., Xu, F., Wang, Y., An, T., Zhang, R., 2019. Interaction between succinic acid and sulfuric acid–base clusters. Atmos. Chem. Phys. 19, 8003–8019.
Liu, L., Zhang, X., Li, Z., Zhang, Y., Ge, M., 2017. Gas-phase hydration of glyoxylic acid: kinetics and atmospheric implications. Chemosphere 186, 430–437.
Liu, Y.-R., Wen, H., Huang, T., Lin, X.-X., Gai, Y.-B., Hu, C.-J., Zhang, W.-J., Huang, W., 2014. Structural exploration of water, nitrate/water, and oxalate/water clusters with Basin-Hopping method using a compressed sampling technique. J. Phys. Chem. A 118, 508–516.
Loukonen, V., Kurtén, T., Ortega, I.K., Vehkamäki, H., Pádua, A.A.H., Sellegri, K., Kulmala, M., 2010. Enhancing effect of dimethylamine in sulfuric acid nucleation in the presence of water – a computational study. Atmos. Chem. Phys. 10, 4961–4974.
Lu, T., Chen, F., 2013. Bond order analysis based on the laplacian of electron density in fuzzy overlap space. J. Phys. Chem. A 117, 3100–3108.
Lv, S.-S., Miao, S.-K., Ma, Y., Zhang, M.-M., Wen, Y., Wang, C.-Y., Zhu, Y.-P., Huang, W., 2015. Properties and atmospheric implication of methylamine–sulfuric acid–water clusters. J. Phys. Chem. A 119, 8657–8666.
Ma, Y., Chen, J., Jiang, S., Liu, Y.-R., Huang, T., Miao, S.-K., Wang, C.-Y., Huang, W., 2016. Characterization of the nucleation precursor (H_2SO_4–$(CH_3)_2NH$) complex: intra-cluster interactions and atmospheric relevance. RSC Adv. 6, 5824–5836.
McGrath, M.J., Olenius, T., Ortega, I.K., Loukonen, V., Paasonen, P., Kurtén, T., Kulmala, M., Vehkamäki, H., 2012. Atmospheric Cluster Dynamics Code: a flexible method for solution of the birth-death equations. Atmos. Chem. Phys. 12, 2345–2355.
Miao, S.-K., Jiang, S., Chen, J., Ma, Y., Zhu, Y.-P., Wen, Y., Zhang, M.-M., Huang, W., 2015. Hydration of a sulfuric acid–oxalic acid complex: acid dissociation and its atmospheric implication. RSC Adv. 5, 48638–48646.
Miao, S.-K., Jiang, S., Peng, X.-Q., Liu, Y.-R., Feng, Y.-J., Wang, Y.-B., Zhao, F., Huang, T., Huang, W., 2018. Hydration of the methanesulfonate–ammonia/amine complex and its atmospheric implications. RSC Adv. 8, 3250–3263.
Nadykto, A.B., Yu, F., Herb, J., 2009. Theoretical analysis of the gas-phase hydration of common atmospheric pre-nucleation $(HSO_4\text{-})(H_2O)_n$ and $(H3O^+)(H_2SO_4)(H2O)_n$ cluster ions. Chem. Phys. 360, 67–73.
Nadykto, B.A., Yu, F., Jakovleva, V.M., Herb, J., Xu, Y., 2011. Amines in the earth's atmosphere: a density functional theory study of the thermochemistry of pre-nucleation clusters. Entropy 13.
Oberdörster, G., Utell, M.J., 2002. Ultrafine particles in the urban air: to the respiratory tract–and beyond? Environ. Health Perspect. 110, A440–A441.
Ortega, I.K., Donahue, N.M., Kurtén, T., Kulmala, M., Focsa, C., Vehkamäki, H., 2015. Can highly oxidized organics contribute to atmospheric new particle formation? J. Phys. Chem. A 120, 1452–1458.
Peterson, K.A., Adler, T.B., Werner, H.-J., 2008. Systematically convergent basis sets for explicitly correlated wavefunctions: the atoms H, He, B–Ne, and Al–Ar. J. Chem. Phys. 128, 084102.
Prenni, A.J., DeMott, P.J., Kreidenweis, S.M., Sherman, D.E., Russell, L.M., Ming, Y., 2001. The effects of low molecular weight dicarboxylic acids on cloud formation. J. Phys. Chem. A 105, 11240–11248.
Saxon, A., Diaz-Sanchez, D., 2005. Air pollution and allergy: you are what you breathe. Nat. Immunol. 6, 223–226.
Wales, D.J., Doye, J.P.K., 1997. Global optimization by Basin-Hopping and the lowest energy structures of Lennard-Jones clusters containing up to 110 atoms. J. Phys. Chem. A 101, 5111–5116.
Wang, C.-Y., Ma, Y., Chen, J., Jiang, S., Liu, Y.-R., Wen, H., Feng, Y.-J., Hong, Y., Huang, T., Huang, W., 2016. Bidirectional interaction of alanine with sulfuric acid in the presence of water and the atmospheric implication. J. Phys. Chem. A 120, 2357–2371.
Wang, L., Khalizov, A.F., Zheng, J., Xu, W., Ma, Y., Lal, V., Zhang, R., 2010. Atmospheric nanoparticles formed from heterogeneous reactions of organics. Nat. Geosci. 3, 238–242.
Wen, H., Huang, T., Wang, C.-Y., Peng, X.-Q., Jiang, S., Liu, Y.-R., Huang, W., 2018. A study on the microscopic mechanism of methanesulfonic acid-promoted binary nucleation of sulfuric acid and water. Atmos. Environ. 191, 214–226.
Wen, H., Wang, C.-Y., Wang, Z.-Q., Hou, X.-F., Han, Y.-J., Liu, Y.-R., Jiang, S., Huang, T., Huang, W., 2019. Formation of atmospheric molecular clusters consisting of methanesulfonic acid and sulfuric acid: insights from flow tube experiments and cluster dynamics simulations. Atmos. Environ. 199, 380–390.
Xie, H.-B., Elm, J., Halonen, R., Myllys, N., Kurtén, T., Kulmala, M., Vehkamäki, H., 2017. Atmospheric fate of monoethanolamine: enhancing new particle formation of sulfuric acid as an important removal process. Environ. Sci. Technol. 51, 8422–8431.
Xu, W., Zhang, R., 2012. Theoretical investigation of interaction of dicarboxylic acids with common aerosol nucleation precursors. J. Phys. Chem. A 116, 4539–4550.
Xu, W., Zhang, R.Y., 2013. A theoretical study of hydrated molecular clusters of amines and dicarboxylic acids. J. Chem. Phys. 139, 11.
Xu, Y., Nadykto, A.B., Yu, F., Herb, J., Wang, W., 2010a. Interaction between common organic acids and trace nucleation species in the earth's atmosphere. J. Phys. Chem. A 114, 387–396.
Xu, Y., Nadykto, A.B., Yu, F., Jiang, L., Wang, W., 2010b. Formation and properties of hydrogen-bonded complexes of common organic oxalic acid with atmospheric nucleation precursors. J. Mol. Struct.: THEOCHEM 951, 28–33.
Yoon, J.-W., Park, J.-H., Shur, C.-C., Jung, S.-B., 2007. Characteristic evaluation of electroless nickel–phosphorus deposits with different phosphorus contents. Microelectron. Eng. 84, 2552–2557.
Yousaf, K.E., Peterson, K.A., 2008. Optimized auxiliary basis sets for explicitly correlated methods. J. Chem. Phys. 129, 184108.
Zhang, R., Khalizov, A.F., Wang, L., Hu, M., Xu, W., 2012. Nucleation and growth of nanoparticles in the atmosphere. Chem. Rev. 112, 1957–2011.
Zhang, H., Kupiainen-Määttä, O., Zhang, X., Molinero, V., Zhang, Y., Li, Z., 2017. The enhancement mechanism of glycolic acid on the formation of atmospheric sulfuric acid–ammonia molecular clusters. J. Chem. Phys. 146, 184308.
Zhang, R., 2010. Getting to the critical nucleus of aerosol formation. Science 328, 1366.
Zhang, R., Li, G., Fan, J., Wu, D.L., Molina, M.J., 2007. Intensification of Pacific storm track linked to Asian pollution. Proc. Natl. Acad. Sci. U.S.A. 104, 5295.
Zhang, R., Suh, I., Zhao, J., Zhang, D., Fortner, E.C., Tie, X., Molina, L.T., Molina, M.J., 2004. Atmospheric new particle formation enhanced by organic acids. Science 304, 1487.
Zhang, R.Y., Khalizov, A., Wang, L., Hu, M., Xu, W., 2012. Nucleation and growth of nanoparticles in the atmosphere. Chem. Rev. 112, 1957–2011.
Zhang, Z.-S., Engling, G., Chan, C.-Y., Yang, Y.-H., Lin, M., Shi, S., He, J., Li, Y.-D., Wang, X.-M., 2013. Determination of isoprene-derived secondary organic aerosol tracers (2-methyltetrols) by HPAEC-PAD: results from size-resolved aerosols in a tropical rainforest. Atmos. Environ. 70, 468–476.
Zhao, J., Smith, J.N., Eisele, F.L., Chen, M., Kuang, C., McMurry, P.H., 2011. Observation of neutral sulfuric acid-amine containing clusters in laboratory and ambient measurements. Atmos. Chem. Phys. 11, 10823–10836.